

# Flow behaviors driven by a rotating spiral permanent magnetic field

X.D. Wang<sup>1</sup>, B.Wang<sup>2</sup>, X.Z.Na<sup>2</sup>, J. Etay<sup>3</sup> and Y.Fautrelle<sup>3\*</sup>

<sup>1</sup> CMO, University of the Chinese Academy of Sciences, Beijing, China

<sup>2</sup> Central Iron and Steel Research Institute, Beijing, China

<sup>3</sup> CNRS/SIMAP/EPM, ENSEEG, BP75, St Martin d'Hères Cedex, France

*Corresponding author: yves.fautrelle@simap.grenoble-inp.fr*

## Abstract

A rotating spiral magnetic field, constructed by a series of permanent magnets, is presented in this study, which is used to drive liquid metal flow. The rotation of such magnetic stirrer can then exert spatial- and tempo- electromagnetic force and drive three dimensional turbulent flow within the liquid metal bulk. Its velocity field was measured via the ultrasonic Doppler velocimetry. Two typical toroidal vortices flow patterns: the secondary flow and the globally axial flow in the meridian plane have been validated, which depends on the several structural and operating parameters, i.e., radius of the liquid metal bulk. The critical transition conditions between these two flow patterns have been discussed according to the experimental results.

## Key words:

magnetic field, electromagnetic stirring, permanent magnet, liquid metal, flow pattern, velocity field

## Introduction

Magnetic fields and electromagnetic forces have long been used to control the flow of solidifying melts and improve microstructures or macrosegregations. The magnetic field can be either exerted by current-carrying coils or by permanent magnets with high magnetic densities. Both of these processes obey similar electromagnetic field theories and are described by the Maxwell equations.

Highly efficient electromagnetic forces can drive liquid metal. Consequently, forced convection in liquid metal can agitate the solutal metallic melt in the liquid zone and the liquid metal among dendrites due to the pressure difference in the mushy zone, which strongly influences the morphology of the crystal growth and the solutal rejection (alloy elements) redistribution.

Vivès et al. [1-3] designed a helical permanent magnetic field to stir a semi-solid melt and mix the secondary phase (i.e., the micrometer-scale particulates within the semi-solid melt) to fabricate metal matrix composites. The theoretical flow patterns of the globally axial circulating flow at the meridian interface were discussed by this author. However, the author neglected one important consideration: the flow pattern described (which was arbitrarily defined and not based on any quantitative study) was not the only possible flow pattern under the different operating conditions of the helical magnetic fields. These references do not detail the distribution of the magnetic field and the quantitative velocity field. The imaginary sketch of the flow structure cannot precisely describe the flow behavior, as shown by our measurement results below.

Therefore, in this paper, a rotating helical magnetic field has been constructed via accumulating a series of small permanent magnets to agitate liquid metal flow. The experiment using GaInSn has been performed in a cylindrical vessel to detect the fluid flow. The main purpose of this study is to quantitatively determine the typical flow patterns, where the flow pattern of the global axial flow is considered beneficial. We also highlight the critical transition conditions between these two flow patterns. These measurements were carried out with an ultrasonic Doppler velocimetry (UDV), an efficient tool for velocity measurement in opaque fluids such as liquid metals.

## Experimental setup and process

### Magnetic field and stirrer

In this paper, a helical permanent magnetic field was constructed using a series of small arc-like magnets to achieve a similar magnetic field structure (figure 1a). To achieve a sufficiently high magnetic impulse, we employed a series of NdFeB magnets of the permanent magnetic material 38UH with a typical remanence of  $B_r=1.22$  T. As shown in Figure 1(b), the inner radius of the arc-like permanent magnet is  $R_1 = 40$  mm, the outer radius is  $R_2 = 70$  mm, the thickness is  $h = 7$  mm, the arc angle is  $\pi/6$  and the magnetization direction is in the radial direction of each unit. The magnetic units were embedded in an aluminum frame to form the unit-structure. As shown in Figure 1(b),  $n$  represents the unit number (here,  $n = 12$  units), and all of the units were installed co-axially at a stagger angle of  $\pi/12$  to the counterclockwise direction of the neighboring unit-structures azimuthal shift. These units eventually form a helical magnetic stirrer as

seen in figure 2. The height of helical magnetic stirrer was  $H = 84$  mm, the wave number was  $k = \pi/H = 0.0375 \text{ mm}^{-1}$ , and the helix lead angle was  $\alpha = \arctan(H/\pi R_2) = 0.36$ .

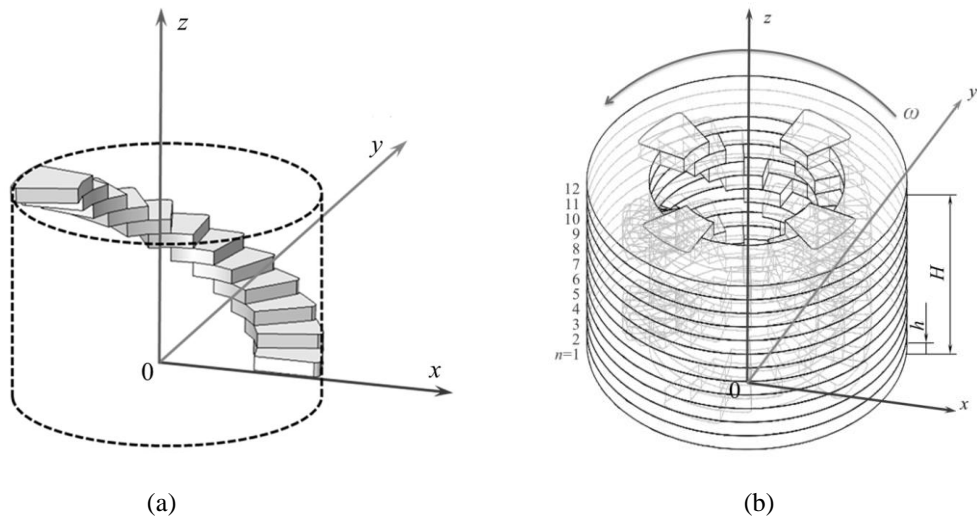


Figure 1. A helical permanent magnet and its construction.

(a) A structure consisting of a series of small permanent magnets; (b) Unit-structure with an aluminum supporting frame;

A frequency converter was used to control the rotating speed of the driving motor, which was connected to the magnetic stirrer by a belt. The frequency range was 1-50 Hz, and its resolution was 0.01 Hz. The angular velocity of the magnetic stirrer can be regulated by adjusting the frequency of this frequency converter. The corresponding angular velocities range from  $\pi$  rad/s to  $16\pi$  rad/s.

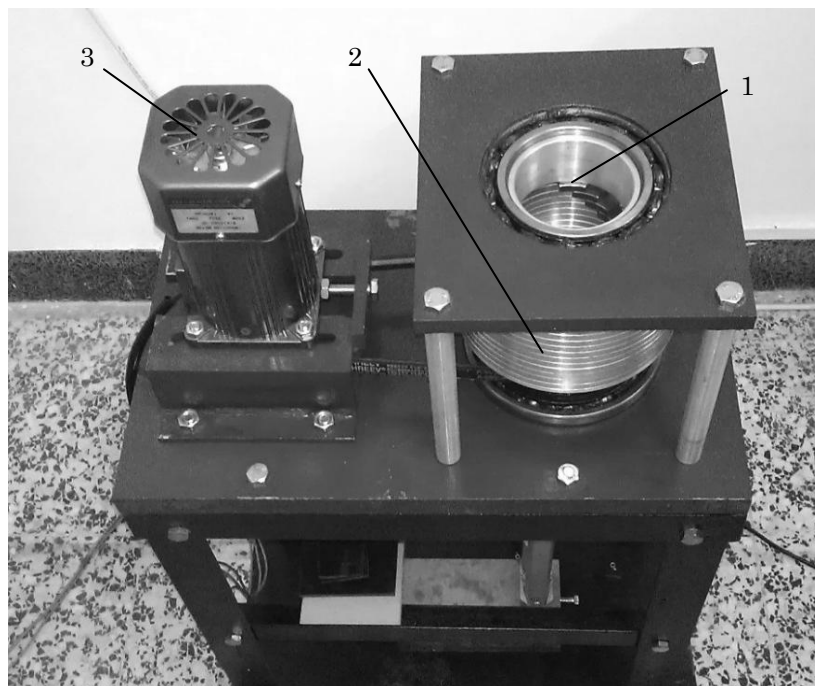


Figure 2. Experimental setup of magnetic stirrer.

1-permanent magnets, 2-stirrer, 3-motor.

### Velocity measurement

The UDV DOP 3010 (Signal Processing SA, Switzerland) was used to measure the velocity field of the liquid metal flow driven by the magnetic stirrer. Two types of 8-MHz cylindrical transducers (TR0805L, size  $\Phi 8 \times 30$  mm and  $\Phi 8 \times 8$  mm, Signal Processing SA, Switzerland) were used. The former was applied to measure the axial velocity while the latter was applied to measure azimuthal and radial velocity according to the different working space. The spatial and temporal resolutions were 0.228 mm and 67 ms, respectively, and the pulse recurrence frequency (PRF) and the sampling volume were set to 400 us and 3.276 mm, respectively. The principle and measuring methodology of the UDV are described in the literature [4-9]. The metallic alloy  $\text{Ga}^{67}\text{In}^{20.5}\text{Sn}^{12.5}$  was used, which has a melting point of  $10.5^\circ\text{C}$  and maintains a liquid state at room temperature. The physical properties of the alloy include an electric conductivity of  $\sigma = 3.2 \times 10^6 \text{ Sm}^{-1}$ , a density of  $\rho = 6.36 \times 10^3 \text{ kgm}^{-3}$  and a kinematic viscosity of  $\nu = 3.4 \times 10^{-7} \text{ m}^2\text{s}^{-1}$ . In this paper, the total height  $H$  of the liquid bulk is fixed at 40 mm for all velocity measurements, while its diameter  $D = 2R$  ranges from 40 mm to 70 mm in an interval of 5 mm. Thus the  $D/H$  ratios are 1, 1.125, 1.25, 1.375, 1.5, 1.625 and 1.75, respectively. We employed a UDV transducer positioning array to investigate the variations of the flow patterns due to the electromagnetic stirrer under different parameters. The flow patterns for dimensions of  $D = 40$  mm,  $H = 40$  mm and  $D/H = 1$  and  $D = 70$  mm,  $H = 40$  mm and  $D/H = 1.75$  were recorded. Thus, the velocity field in a certain vertical cross-section  $y = 0$  can be obtained for ( $D/H = 1$ ) and ( $D/H = 1.75$ ).

### The measured results

#### Flow patterns

The measured results demonstrate that the variation of the flow patterns depends on the dimensions, particularly the diameter, of the cylindrical liquid metal bulk. This result implies a change in the spatial distribution of the Lorentz force. When  $D/H = 1$  (figure 3(a)), the azimuthal component of the Lorentz force played a dominant role because the liquid bulk is far from the permanent magnets, making the axial component smaller. When  $D/H = 1.75$  (figure 3(b)), the diameter of the liquid bulk increases, thus the axial component of the Lorentz force may become stronger than that of the azimuthal component. We will discuss the transitions between secondary and global axial flow in the next section.

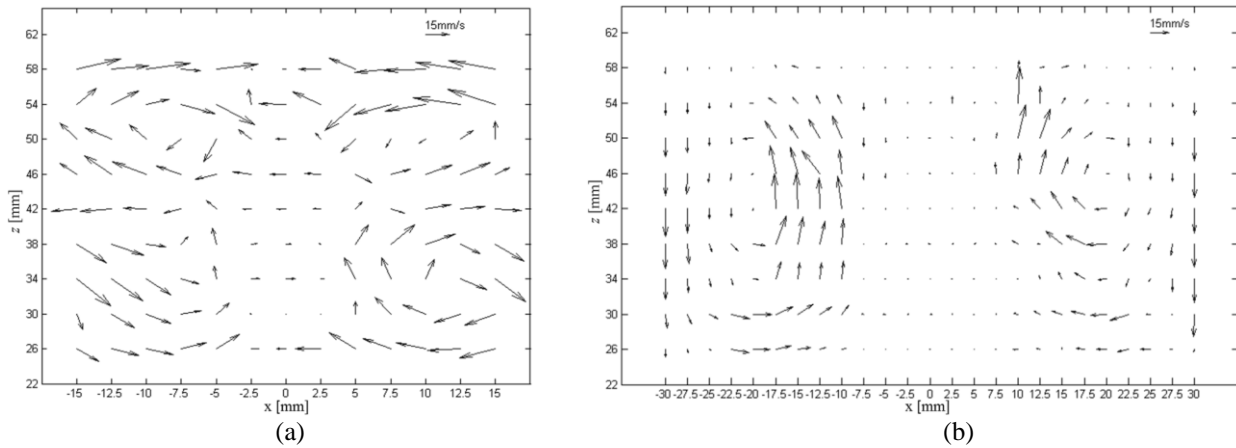


Figure 3. Meridian vector velocity fields at the cross-section  $y = 0$  indicating the flow patterns of meridian (a) secondary flow ( $D/H = 1$ ) and (b) global axial flow ( $D/H = 1.75$ ) driven by an electromagnetic stirrer.

#### Transition between the two flow patterns

Some researchers have studied the transition between secondary and global axial flow patterns according to the type of current-carrying coils in the electromagnetic field [10-13]. The azimuthal and axial component forces can be expressed by the electric conductivity, initial magnetic flux density and other parameters of the magnetic stirrer.

The transition can be characterized by the ratio relationship of the diameter and height of the liquid bulk. Figure 4 shows that as  $D/H$  increases, the axial component of the magnetic flux density increases faster than that of the azimuthal component, and the liquid metal gradually transforms from the meridian secondary flow to the global axial flow. The meridian secondary flow plays a dominant role when  $D/H \leq 1.25$ , whereas the global axial flow dominates when  $D/H \geq 1.375$ . The transition occurred at  $1.25 < D/H < 1.375$ .

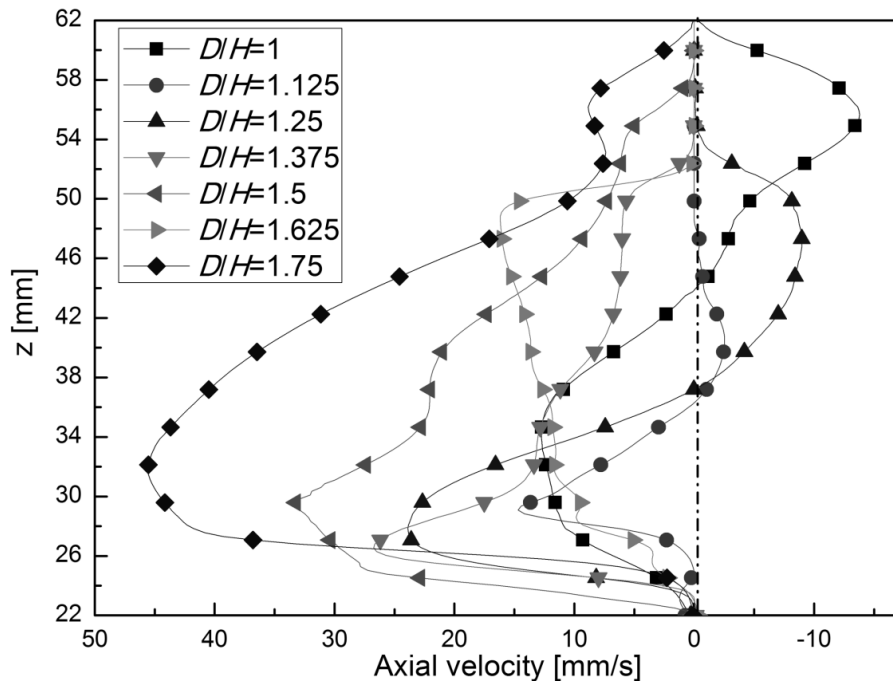


Figure 4. Transitions between the meridian secondary flow and the global axial flow.

### Conclusions and perspectives

This study has experimentally investigated the liquid metal behaviors in a cylindrical vessel exposed to a helical permanent magnetic field. Using a standard UDV technique, the velocity field and its variation were measured. We obtained two typical flow patterns by changing the bulk diameter-to-height ratio and discussed the transitions between these two flow patterns. Such flow patterns study can then be served as the design and optimization of magnetic field using for improving solidification defects such as macrosegregations.

### Acknowledgment

The authors acknowledge the support of the Chinese Academy of Sciences (CAS) in the form of the "One Hundred Talented People" program and CAS funding (XDA04078400).

### References

- [1] C.N. Vives, J. Bas, G. Beltran, G. Fontaine (1993), Mater. Sci. Eng., 173, 239-242
- [2] C.N. Vives (1993), Metall. Trans. B, 24B, 493-510
- [3] C.N. Vives (1996), Magnetohydrodynamics, 32, 201-206
- [4] D. Raebiger, S. Eckert, G. Gerbeth (2010), Exp. Fluids., 48, 233-244
- [5] O. Andreev, Y. Kolesnikov, A. Thess (2009), Exp. Fluids., 46, 77-83
- [6] S. Eckert, G. Gerbeth (2002), Exp. Fluids., 32, 542-546
- [7] S. Eckert, B. Willers, G. Gerbeth (2005), Metall. Mater. Trans. A, 36A, 267-270
- [8] H. Kikura, Y. Takeda, T. Sawada (1999), J. Magn. Magn. Mater., 201, 276-280
- [9] Y. Takeda (1995), Exp. Therm. Fluid. Sci., 10, 444-453
- [10] A. Cramer, J. Pal, G. Gerbeth (2007), Phys. Fluids., 19, 118109-1-4A
- [11] A. Cramer, J. Pal, K. Koal, S. Tschisgale, J. Stiller, G. Gerbeth (2011), J. Cryst. Growth, 321, 142-150
- [12] C. Zhang, V. Shatrov, J. Priede, S. Eckert, G. Gerbeth (2011), Metall. Mater. Trans. B, 42B, 1188-1200
- [13] I. Grants, C. Zhang, S. Eckert and G. Gerbeth (2008), J. Fluid. Mech., 616, 135-152